Optimization and Evaluation of qPCR Duplex Assay for mtDNA Copy Number Quantification

Gretchen Johnson, B.S.[1], Nicole Phillips, Ph.D.[1], John V. Planz, Ph.D.[1]
[1]*Department of Microbiology, Immunology, & Genetics, University of North Texas Health Science Center, Fort Worth, TX, USA*

I. Abstract:

Purpose: The mitochondrial genome (mtDNA) encodes thirteen essential proteins in oxidative phosphorylation, the cell's primary energy-generating process. Depending on the cell type and stage of development, each cell contains an average of 10^3 to 10^4 copies of mtDNA. Current methods of quantification of mtDNA copy number can be imprecise due to low efficiencies of assays and inherent imbalance of mtDNA copy number with nuclear DNA (nDNA) copy number. Accurate quantification of both mtDNA and nDNA is important when calculating the ratio of mtDNA to nDNA. The goal of this project is to optimize a duplex assay that will give precise and accurate estimates in human samples.

Methods: Here we employ **s**ynthetic oligomer standards for an absolute real-time qPCR assay. The significance of using absolute qPCR is that the standard curve allows for the direct comparison of unknowns to obtain a copy number. The mitochondrial target is a site in the minor arc (MinArc), and the nuclear target is a single copy locus (β2M). The accuracy of this assay was evaluated using a standard reference material (SRM2372a) and the precision was evaluated via replications.

Results: This design resulted in high R^2 values for the standards as well as sufficiently high efficiencies. The precision of the assay was analyzed over 6 replicated runs and was deemed effectively reproducible. The accuracy was assessed with the use of a standard reference material (SRM 2372a) and was found to be problematic [**Romsos et al., 2018**]. This could be from a possible dilution bias of the SRM, effectively changing the copy number ratios in a difficult to predict way [**Malik et al., 2011**]. An attempt to mathematically correct the data was made but did not provide any solution.

Conclusion: The optimization of this assay is ongoing due to the error in accuracy. The assay has proven to be precise and reproducible with sufficient efficiency. Possible future directions include sonication of samples and SRMs to examine if dilution bias could be the cause of inaccurate SRM quantification. Other methods of possibly reducing dilution bias mentioned in Malik *et al*. [**2011**] include manual shearing and the use of DNA carriers such as tRNA. Another avenue of future research could include a different method of mathematically correcting the data post run to improve accuracy. This assay has the potential to provide data which can be used to indicate overall mitochondrial health and can be utilized in various research areas such as aging, cancer, forensics and neurodevelopment.

II. Introduction:

Mitochondria are known for being the cell's primary energy-generating source, accomplished through the process of oxidative phosphorylation via the electron transport chain. The organelle also has its own circular genome of approximately 16 kilobase pairs and is maternally inherited. The mitochondrial genome (mtDNA) encodes thirteen of the essential protein subunits that are used in oxidative phosphorylation [**Andreu et al., 2009; Bai et al., 2004; Jayaprakash et al., 2015**]. Depending on the cell type and stage of development, each cell contains an average of 10^3 to 10^4 copies of mtDNA [**Rooney et**

al., 2014]. Replication of mtDNA can be highly variable relative to the cell-type's energy demand and the genome is susceptible to mutations caused by reactive oxygen species continually being produced during respiration [**Dennenmann et al., 2017; Wallace, 2010**]. There is inherent variability in the amount of both mitochondria per cell and mtDNA per organelle because of those differences in energy needs of the many cell types. The amount of mtDNA compared to the amount of nuclear DNA (nDNA) can be referred to as "mtDNA content" and is often a subject of interest in mitochondrial research [**Bai et al., 2004**]. There are only two copies of nuclear DNA per cell so there is an innate imbalance in copy number, but in terms of base pairs the amount of nuclear base pairs far exceeds that of mitochondrial base pairs. These dynamics contribute to the difficulty in specific amplification of mtDNA in the presence of nDNA. [**Phillips et al., 2014; Decker et al., 2005**].

It has long been observed that mtDNA content not only varies across tissue types but across individuals [**Shmookler Reis & Goldstein, 1983; Bai et al., 2004**]. Shmookler Reis and Goldstein [**1983**] examined mtDNA content per picogram of protein and observed variation in fibroblasts between individuals. Bai *et al.* [**2004**] reviewed reports of mtDNA content between individuals of different ages and different tissues (skeletal muscle and blood) and found broad variation as well as a correlation between abnormal levels of mtDNA with clinical manifestations of phenotypes associated with mitochondrial disease. There have also been reports of changes in mtDNA content across other human diseases including diabetes, obesity, cancer, HIV complications, and aging [**Malik & Czajka, 2013**]. It has been established that there is a variation in observed mtDNA content values per individual and per population and that there are changes with regards to mitochondrial dysfunction diseases as well as other diseases. It is hypothesized that the relationship between nuclear DNA copy number and mitochondrial DNA copy number is driven by the cell's energy production needs [**Bai et al., 2004; Jayaprakash et al., 2015; Malik & Czajka, 2013; Shmookler Reis & Goldstein, 1983**]. However, uncertainty in the driving force behind depletion or proliferation of mtDNA content and resulting disease phenotypes remains. This underlines the need for further research utilizing methods of obtaining mtDNA content data with regards to disease etiology. Interestingly, Malik & Czajka [**2013**] reported that across the many studies they reviewed data often conflicted between papers, which was attributed to current methodology giving false results. The authors gave the following as possible explanations for false results: mitochondrial primers that co-amplify nuclear pseudogenes; use of nuclear genes that are variable and/or duplicated as targets; dilution bias caused by the differing genome sizes; and template preparation protocols affecting yield of nuclear and mtDNA. The term dilution bias was used in Malik *et al.* [**2011**] to describe an observed difference in expected dilution results, which the authors theorized was due to the difference in molecular weight and size of the two genomes.

The process of DNA quantification has improved significantly over the years. Traditionally, estimates were made based on band intensity in gel electrophoresis and analyzed with Southern blot hybridization [**Shmookler Reis & Goldstein, 1983**]. Then, advances in spectrophotometry allowed for the difference in light absorption to indicate quantity more precisely. With the development of polymerase chain reaction (PCR) came even more methods of quantifying DNA. Real-time PCR, also known as quantitative PCR (qPCR), combines fluorescence detection with controlled amplification to provide even more accurate results and allow for the monitoring of the reactions in real time. TaqMan™ qPCR makes use of a fluorescent probe that attaches to a target sequence in a sample and the fluorescence is stifled while attached to DNA due to a non-fluorescent quencher. As the elongation step occurs, the probe is displaced from the quencher and DNA and then is able to give off fluorescence directly correlating with the amount of sample being elongated at that time. Specificity of primers and probes are vital and so the

design of these components play a big role in the efficiency of the assay. Efficiency is determined by the slope of the standard curve, which is indicative of polymerase function. An efficiency of 100% corresponds to fluorescence doubling each cycle, and a more gradual slope from non-exponential amplification will cause efficiency to drop below 100%.

There are two primary ways to analyze qPCR data: absolute quantification and relative quantification. Absolute quantification of any kind is determining input copy number or absolute transcript copy number, and this is done by relating the PCR signal of unknowns to the PCR signal of a standard curve. Absolute qPCR therefore utilizes standards to evaluate samples and estimate input amount. Relative quantification relates the PCR signal of a target sequence in a treatment group to the PCR signal of another sample (e.g. different treatment group, untreated control) to record change in expression. Relative qPCR therefore uses a reference gene or sample to relate to a treated sample and the quantity is measured as fold changes from before treatment to after. [**Livak & Schmittgen, 2001**]

When qPCR is used with a single target, it is easier to add the specific primers and probe to a PCR master mix and have expected amplification occur than when multiple targets are used. A multiplex reaction interrogates multiple targets in a simultaneous reaction by use of probes with different emission wavelengths. Multiplexing is more complicated because the master mix contains multiple sets of primers and probes that are competing for components, such as dNTPs, to amplify both targets simultaneously. The specific composition of the master mix is essential because different targets can have different affinities for reagents and if there is more of one type of target than the other, then it can be favored in the reaction and give inaccurate results of the other target. Multiplex assays often lead to reduced efficiency compared to the singleplex assays [**Decker et al., 2005**]. A contributing factor is PCR bias, which is when one set of primers is favored over the other due to the binding energy. Kanagawa [**2003**] concluded that PCR bias can be minimized through replications of PCR and by stopping the reaction several cycles early. Another issue to be aware of is compatible melting temperatures of primers as well as possible primer-primer and primer-probe interactions that hinder expected amplification [**Phillips et al., 2014**].

The accuracy of an assay is determined by use of references and validation studies that address the reliability of the results and references. The precision of an assay is determined through replicates and analysis of observed variance. At lower concentrations and low copy number, precision varies more than it does at higher concentrations. This is why repeatability of an assay should be assessed by standard deviation errors or confidence intervals. There are two types of variation that should be addressed: the variation of the assay itself and the variation between samples. Technical variation of an assay is assessed by replicating results of the same sample however, it does not account for biological variation when population samples are used in practice. Biological variation is measured by biological replicates which can give statistical significance to the observed differences between groups. Biological replicates are different samples of the same type, such as saliva samples from 10 different individuals. [**Bustin et al., 2009**]

There have been several multiplex assays developed for the measurement of mtDNA and nDNA to obtain a ratio estimate for calculating copy number (**Table 1**). Multiplex assays that are designed to observe mtDNA content have proven difficult to optimize due to needed changes in amplification conditions for mitochondria specific primers and probe to work along with nuclear primers and probe. In addition, because of the variability of mitochondrial copy number per sample it is challenging to obtain consistent mtDNA/nDNA ratios in a population group and across studies [**Decker et al., 2005; Malik & Czajka, 2013**]. The assays in **Table 1** suffer from some of the issues Malik & Czajka [**2013**] mentioned

regarding specificity of the mitochondrial primers, possible multiple copies of the nuclear target, dilution bias in standards, and variation in the template preparation. Alonso *et al.* [**2004**] created a mitochondrial only duplex that quantified two different sized targets in the HVI region of the control region and a separate assay that quantified the nuclear target on Amelogenin, and then found mtDNA content from the ratio of the separate reactions. Not only is this not an ideal design due to the separate reactions, but the efficiencies were not ideal, the authors stated the need for further studies on determining reproducibility, and the standards were serial dilutions from samples which would be afflicted by dilution bias. Andréasson *et al.* [**2002**] designed an assay with a unique mitochondrial target in the ATPs8 gene and a nuclear target in RB1 gene on chromosome 13 also using a standard dilution series but from genomic and cloned mtDNA, which would still be affected by dilution bias. Andréasson *et al.* [**2006**] noted that they used the assay as two singleplex reactions to increase the efficiency since the duplex was insufficient. Andreu *et al.* [**2009**] used a commercial kit to quantify nuclear target RNaseP and separately quantified the mitochondrial target in the 12s rRNA region. The authors used a calibration curve calculated from serial dilution of plasmids, which was later theorized to result in absolute quantification errors [**Phillips et al., 2014**]. Bai *et al.* [**2004**] chose a region in the mitochondrial genome that is in both the 16s rRNA and ND1 regions and a nuclear target of the 18s rRNA gene. The standard curve was generated by a serial dilution of PCR products of a cloned vector. Kavlick [**2011**] designed an assay that was used by other authors including Bintz & Wilson [**n.d.**] that utilized a mitochondrial target in the ND5 region and a mobile element for the nuclear target, *Alu* Yd6. While this nuclear target is not a single copy gene, as is recommended by Malik & Czajka [**2013**], it had been used previously and Kavlick [**2011**] claims the multiplex has similar efficiency to the singleplex. Timken *et al.* [**2005**] designed an assay with a mitochondrial target in the ND1 region, TH01 as the nuclear target, and synthetic oligonucleotide standards. The authors specified that they used optimal conditions for TH01 amplification and limited conditions for mtND1, which could result in an underestimation of mtDNA in samples that are more robust in nuTH01 causing lower efficiency of mtND1 amplification. Wurmb-Schwark [**2004**] also used a mtDNA target in the ND1 region but opted to target the nuclear betaglobin gene BCL-2. This paper did not mention the use of standard curves, only internal standards. A multiplex assay developed by Phillips *et al.* [**2014**] attempted to quantify two targets on mtDNA as well as a nuclear target to obtain both copy number and an idea of the percentage of genomes that contain a common large deletion indicative of oxidative damage. One of the mitochondrial targets is a range of nucleotides in what is called the minor arc (**Figure 1**), where large deletions are rare, and was shown to have relatively high efficiency when used with the single-copy nuclear locus β2M [**Phillips et al., 2014**]. The protocol design below heavily pulls from this assay and utilizes the same primers and probes for one of the two mitochondrial targets (Minor Arc) and the nuclear target (β2M). Dilution bias of standards is accounted for by using synthetic copies of the targets that are similar in both size and shape.

Table 1. Multiplex Assays in Literature

Mitochondrial Target	Nuclear Target	Standards	References
HV1	AMG	Samples	Alonso *et al.*, 2004
ATPs8	RB1	Genomic and cloned	Andréasson *et al.*, 2002
12s rRNA	RNaseP	Plasmid	Andreu *et al.*, 2009
16s rRNA / ND1	18S rRNA	Cloned vector	Bai *et al.*, 2004
ND5	Alu YD6	Synthetic	Kavlick *et al.*, 2011
Minor Arc	β2M	Peripheral Blood Samples	Phillips *et al.*, 2014
ND1	TH01	Synthetic	Timken *et al.*, 2005
ND1	BCL-2	Internal	Wurmb-Schwark *et al.*, 2002

Comparison of various multiplex assays' mitochondrial targets, nuclear targets, and the type of standard used.

Figure 1. Location of mitochondrial targets [Phillips et al., 2014]

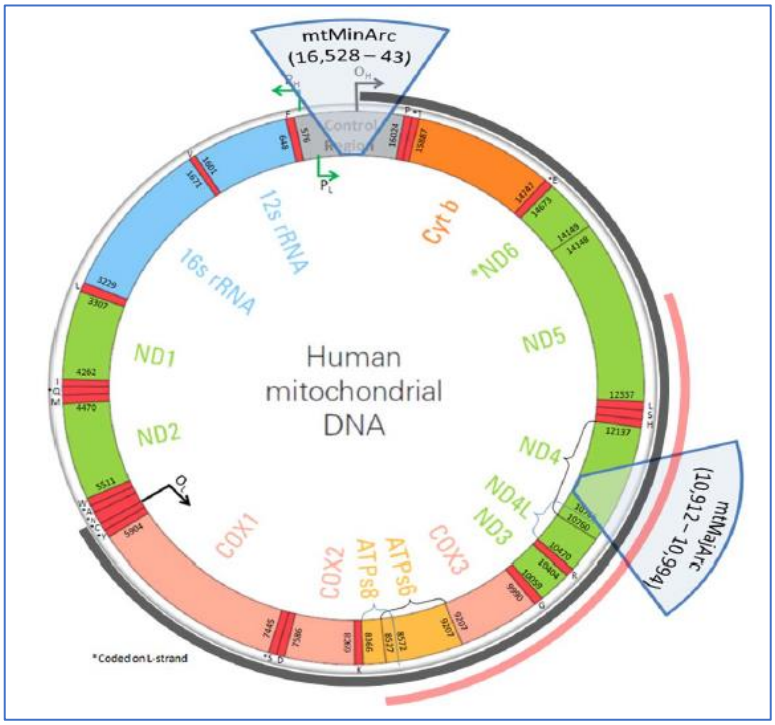

Human mitochondrial DNA from Phillips *et al.* [**2014**]. The target used here is "mtMinArc", nucleotide position 16,528-43, located in the D-loop of the mtDNA where no deletions have been reported.

III. Methodology:

The internship project design is heavily influenced by the protocol developed by Phillips *et al*. [**2014**] and utilizes the same primers and probes for the mitochondrial minor arc and the nuclear β2M locus (**Table 2**). The DNA standards consist of two separate synthetic double-stranded oligomers containing the target sequences that are to be used in the same reaction tube with no cross interaction (**Table 3**). A summary flowchart of the research design is displayed in **Figure 2**.

Table 2. Primer and Probe Design

Name	Specificity	Binding Site Positions	Sequence
MinArcF Primer	mtDNA	mt 16,528 – 16,548	5'CTAAATAGCCCACACGTTCCC-3'
MinArcR Primer	mtDNA	mt 23 – 42	5'AGAGCTCCCGTGAGTGGTTA-3'
MinArc Probe	mtDNA	mt 16,560 – 10	6FAMCATCACGATGGATCACAGGTMGBNFQ
β2MF Primer	nDNA	Chr15 15,798,932 – 15,798,958	5'GCTGGGTAGCTCTAACAATGTATTCA-3'
β2MR Primer	nDNA	Chr15 15,798,999 – 15,799,026	5'CCATGTACTAACAAATGTCTAAAATGGT-3
β2M Probe	nDNA	Chr15 15,798,969 – 15,798,984	6VICCAGCAGCCTATTCTGCMGBNFQ

Primer pairs and probes names, target, binding site positions, and sequences.

Table 3. gBlock Sequences

gBlock	Sequence
MinArc	CAATCCAATCGGCATCAACCACTAAATAGCCCACACGTTCCCCTTAAATAAGACATCACGATGGATCACAGGTCTATCACCCTATTAACCACTCACGGGAGCTCTACCTTAACAATGAACAGAACA
β2M	CAATCCAATCGGCATCAACCAGCTGGGTAGCTCTAAACAATGTATTCATGGGTAGGAACAGCAGCCTATTCTGCCAGCCTTATTTCTAACCATTTTAGACATTTGTTAGTACATGGACCTTAACAATGAACAGAACA

Sequences of the gBlock synthetic standards (read 5' → 3'), underlined base pairs (bp) are synthetic tags added on both ends of target sequence to reach desired length. MinArc is 126bp and β2M is 137bp.

Figure 2. Flowchart of Experimental Design

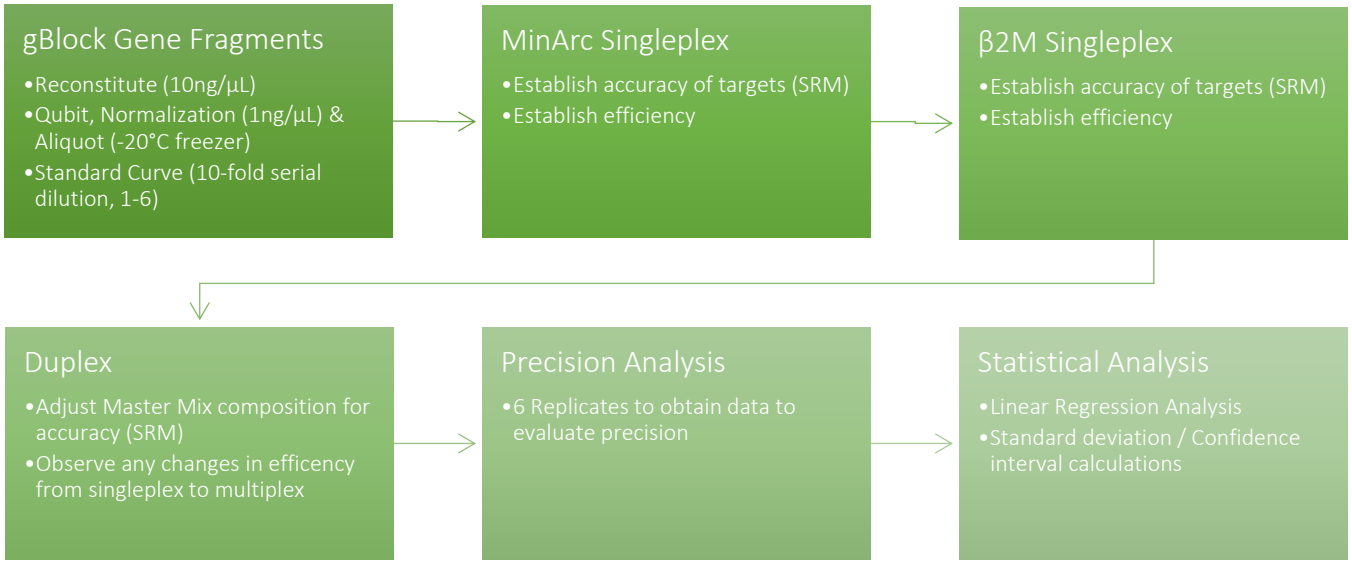

Flowchart depicting each step of the experimental design. gBlock reconstitution and normalization to create standards to be used downstream, Singleplex reactions for each target, Duplex assay and optimization, precision analysis, followed by statistical analysis.

gBlock Gene Fragments

The "gBlock Gene Fragments" were purchased from Integrated DNA Technologies and received dry at approximately 250 nanograms (ng). They were reconstituted per manufacturer instruction to obtain a theoretical concentration of 10 nanograms per microliter (ng/µL), this was considered the primary, 1˚, stock. The actual concentration of each gBlock stock was determined by Qubit Fluorometric Quantification (ThermoFisher Scientific) and then normalized to a concentration of 1ng/µL (MinArc and β2M). The normalized concentrations were the secondary, 2˚, stock and aliquoted into 15 tubes containing 5µL each and stored in a -20°C freezer. Aliquoting the gBlocks allows for minimization of freeze-thaws which can compromise the gBlock integrity. If stored at concentrations lower than 1ng/µL, the gBlocks can irreversibly bind to the tube. Copy number of each standard was calculated using www.scienceprimer.com Copy Number Calculator for real-time PCR based on the molecular weight of the MinArc gBlock and β2M gBlock, 77724.4 and 84515.8 respectively. It was calculated that 0.1ng/µL of β2M would have approximately 7.125E8 copies per µL and the 2˚ MinArc stock would have approximately 7.749E9 copies per µL. To get to the ideal concentration of 0.1ng/µL for β2M, a tertiary (3°) stock needed to be made fresh each assay by taking 2µL of the 2˚ β2M into 198µL of low TE. To create Standard 1, 3.79µL of 2˚ MinArc gBlock and 2.06µL of 3˚ β2M gBlock were added to 494.15µL of low TE, vortexed and spun down. Standard 1 contained approximately 58,800,000 copies of MinArc and 294,000 copies of β2M. Standards 2 through 8 were a 10-fold serial dilution, so 10µL of the previous standard were added to 90µL of low TE, vortexed and spun down (**Table 4**).

Table 4. Standard Curve Dilution Series				
Standard	Copy Number mtDNA / nDNA	TE^{-4} Amount (µL)	DNA Amount (µL)	Dilution Factor
STD 1	58,800,000 / 294,000	494.15µL	2.06 µL 3˚ B2M 3.79µL 2˚ MinArc	-
STD 2	5,880,000 / 29,400	90µL	10µL STD 1	10X
STD 3	588,000 / 2,940	90µL	10µL STD 2	10X
STD 4	58,800 / 294	90µL	10µL STD 3	10X
STD 5	5,880 / 29.4	90µL	10µL STD 4	10X
STD 6	588 / 2.94	90µL	10µL STD 5	10X
STD 7	58.8 / 0.294	90µL	10µL STD 6	10X
STD 8	5.88 / 0.0294	90µL	10µL STD 7	10X
Shows the copy number values for each standard and the amount of low TE and DNA input into each.				

Standard Reference Material 2372a

The use of a standard reference material (SRM) was employed to determine accuracy. The National Institute of Standards and Technology (NIST) certified SRM2372a Human Quantitation Standard for use in value assignment in human DNA quantitation materials. There are three components that are derived from a single male donor, a single female donor, and a 1:3 mixture of a male and a female donor, respectively labeled A, B, and C. Each component contains approximately 55µL of DNA solution. The mtDNA to nDNA ratios for A, B, and C are respectively 174 ± 4, 206 ± 5, and 279 ± 7. In the singleplex reactions, the accuracy was assessed by plating each SRM component in duplicate at a concentration of 0.5ng/µL and observing if the generated copy number was within the certified ranges published. In the duplex reactions, the accuracy was assessed similarly but with concentrations of 25ng/µL, 15ng/µL, 10ng/µL, 5ng/µL, and 2.5ng/µL. [**Romsos et al., 2018**]

MinArc & β2M Singleplex

To confirm that the gBlock standards work as expected with the respective primers and probe, singleplex reactions were done with the MinArc standard and the β2M standard. Singleplex reactions also allow for individual efficiency and accuracy to be determined so that when run in duplex any changes can be taken into consideration for adjusting the master mix composition. Stock primers and probes were all received at concentrations of 100µM from ThermoFisher Scientific. Both the MinArc and the β2M singleplex assays used the same master mix compositions for initial runs and were adjusted as needed. The initial singleplex master mix consists of (per reaction) 12.5µL of *Taq* Universal Master Mix (ThermoFisher Scientific), 4µLof the forward and reverse primers at concentrations of 5µM, and 2.5µL of the probe at a concentration of 2.5µM. The total plate volumes were calculated each run based on the number of reactions and include 10% overage. The standards were run in duplicate with two non-template controls (NTC) of low TE and then each SRM component (at 5ng/µL) in duplicate. Each well contained 23µL of master mix and 2µL of either standard, NTC, or SRM. The assays were run on the Applied Biosystems 7500 Real-Time PCR instrument. qPCR cycling parameters used were 1 cycle at 95ºC for 10 minutes (stage 1), followed by 40 cycles of 95ºC for 15 seconds, 55ºC for 15 seconds, and 60ºC for 1 minute (stage 2) with data collection happening in stage 2 step 3 (60ºC for 1 minute).[**Phillips et al., 2014]**. There were a total of 5 MinArc singleplex assays and 3 β2M singleplex assays run to obtain data.

Duplex & Precision

To combine MinArc and β2M for the duplex assay, the initial master mix composition was similar to the singleplex master mixes with total primer volumes of 4µL and probe volumes of 2.5µL per reaction. To do this, the master mix consisted of (per reaction) 12.5µL of *Taq* Universal Master Mix (ThermoFisher Scientific), 2µLof the forward and reverse primers at concentrations of 10µM, and 1.25µL of each probe at a concentration of 5µM. Again, the total plate volume was calculated each run based on the number of reactions and include 10% overage with standards, NTCs, and SRMs being run in duplicate. Each well had 23µL of master mix and 2µL of either standard, NTC, or SRM. The assay was run on the Applied Biosystems 7500 Real-Time PCR instrument. qPCR cycling parameters used were 1 cycle at 95ºC for 10 minutes (stage 1), followed by 40 cycles of 95ºC for 15 seconds, 55ºC for 15 seconds, and 60ºC for 1 minute (stage 2) with data collection happening in stage 2 step 3 (60ºC for 1 minute).[**Phillips et al., 2014]**. The per reaction master mix volume was 23µL with 12.5µL of the *Taq* Universal Master Mix (ThermoFisher Scientific) and to optimize the concentrations of primers and probes were adjusted. The final composition used was 12.5µL of *Taq* Universal Master Mix (ThermoFisher Scientific), 2µL of β2M primers at 7.5µM, 1.25µL of β2M probe at 4µM, 2µL of MinArc primers at 625nM, and 1.25µL of MinArc probe at 2µM. A total of 12 duplex assays were run, 6 of which are replicates of finalized procedure to assess precision.

Statistical Analysis

The statistical analyses performed includes linear regression analysis of the standard curves for efficiency and calculating standard deviation from replicate data for precision. To confirm the assay was working as expected and performing accurately, the copy number values of the SRM components were assessed and compared to the certified values.

IV. Results:

MinArc Singleplex

The average efficiency of the MinArc singleplex assays was approximately 85%, **Figure 3a**. shows a representative curve and the lowest quantity standard (#8) shows deviation from the line of best fit resulting in an R^2 value of 0.991. The amplification of standards is shown in **Figure 3b.**, baseline threshold was set at 0.2 for the software to analyze slope.

Figure 3a. MinArc Linear Regression Analysis

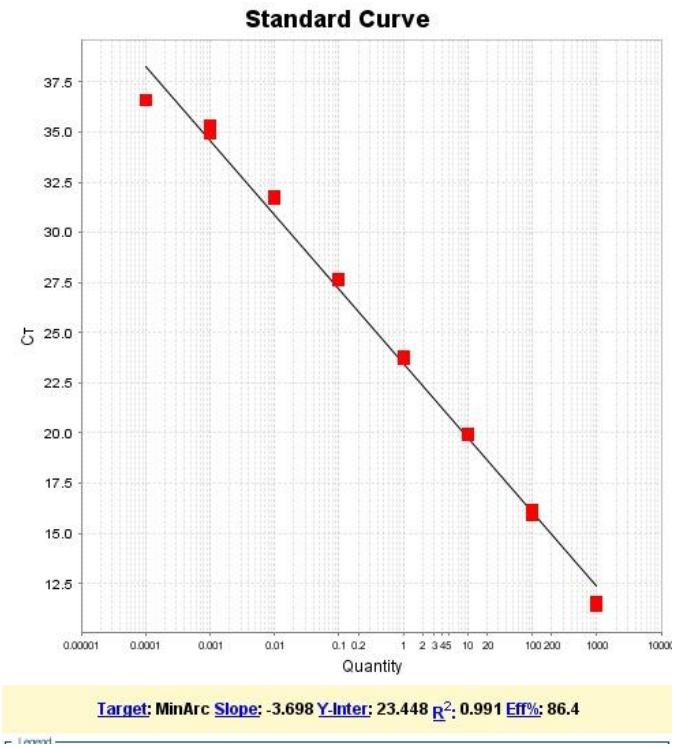

10X Dilution series of MinArc gBlock Standards.

Figure 3b. MinArc Amplification Plot

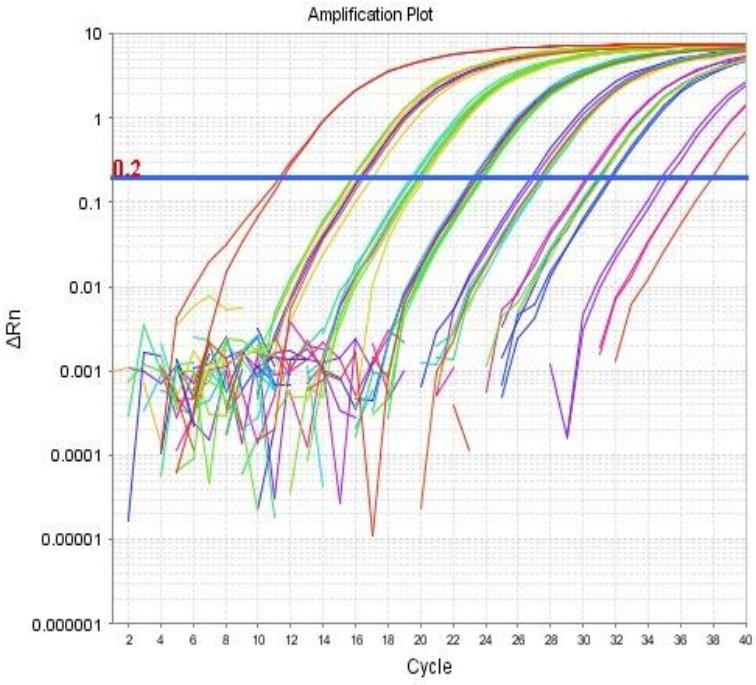

Per cycle amplification, the lower the cycle number for amplification the higher the quantity of sample or standard.

β2M Singleplex

The average efficiency of the β2M singleplex assays was approximately 91%, **Figure 4a.** shows a representative curve with only the first 6 standards. Standards 7 and 8 were excluded because the extremely low copy numbers either did not quantify or stochastically quantified, deviating from the line of best fit. R^2 value of standards 1-6 was at 0.993. The amplification of nuclear standards is shown in **Figure 4b.**, baseline threshold was set to 0.1 for analysis of slope.

Figure 4a. β2M Linear Regression Analysis

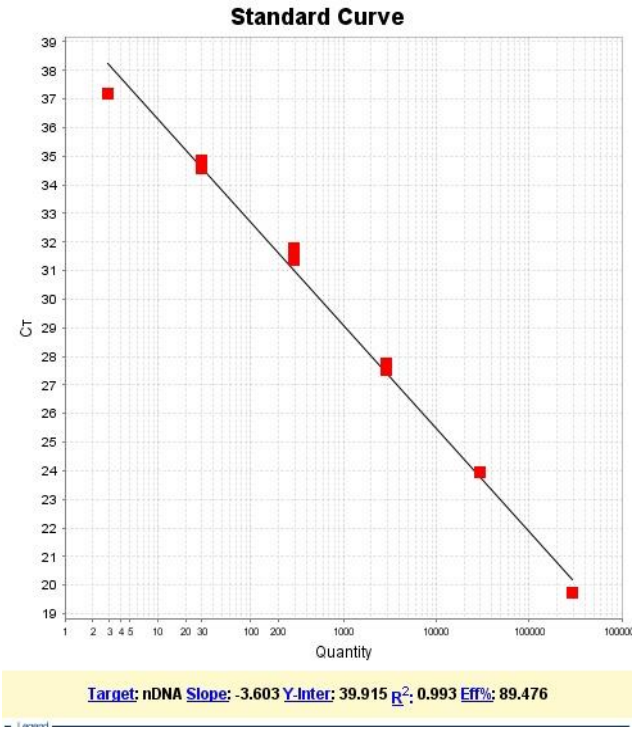

10X Dilution series of β2M gBlock Standards

Figure 4b. β2M Amplification Plot

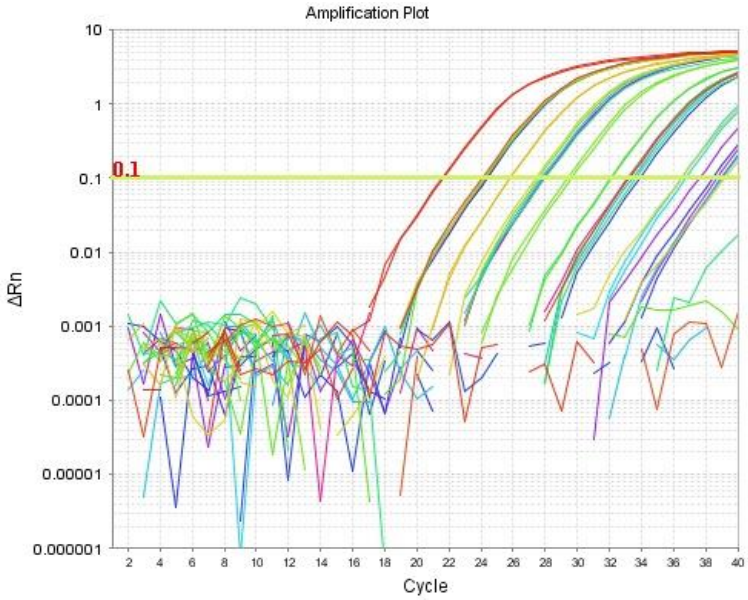

Per cycle amplification, the lower the cycle number for amplification the higher the quantity of sample or standard.

Duplex & Precision

The first 3 duplex runs were used for adjusting the master mix composition. Run 4 was intended to replicate run 3 data but showed a shift in cycle threshold for β2M to the right, indicating a decrease in copy number (**Figure 5.**). Run 5 tested different methods of preparing the standards, one set prepared the same as the previous run, one set vortexed right before plating, and one set heated to 95ºC for 2 minutes prior to creation and vortexed right before plating. There were no significant differences found, indicating decrease in quantity was caused by something else. On the gBlock Gene Fragment's manufacturer "Frequently Ask Questions" page it was noted that storing gBlocks at concentrations lower than 1ng/µL could result in a decrease in concentration due to the fragments irreversibly binding to the tube, even in low bind tubes. At this point the MinArc was being stored at 1ng/µL and B2M was being stored at 0.1ng/µL. To test if this was the cause, new stock B2M was made and stored at 1ng/µL and diluted to 0.1ng/µL only right before making the standards. Run 6 showed that the new gBlocks were quantifying closer to the expected cycle threshold, and so all subsequent runs incorporated the new gBlock storage method.

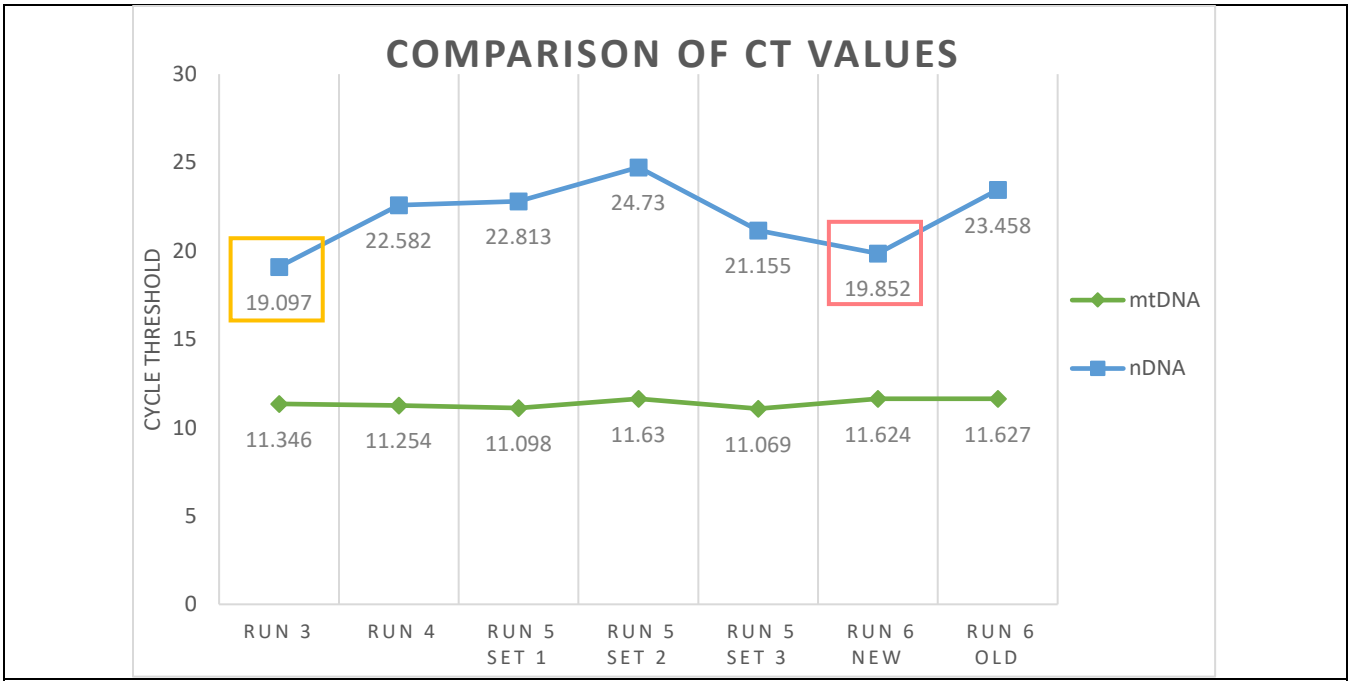

Figure 5. mtDNA cycle threshold values shown in green and nDNA cycle thresholds shown in blue. This is a comparison of just the first standard in each of the specified runs to illustrate the change in concentration of nDNA. The gold box highlights the ideal cycle threshold. The red box highlights the standards that were remade to test if storage concentration was the cause of decreasing quantity / increasing cycle threshold.

Runs 7 through 12 were the replicates of the finalized methodology. A representative of the standard curves is shown in **Figure 6a.**, with an R^2 value of 1 and an average efficiency of 86.9% for MinArc, and 87.3% for β2M. The amplification of both targets is demonstrated in **Figure 6b.** with thresholds at 0.1 for β2M and 0.2 for MinArc.

Figure 6a. Duplex Linear Regression Analysis	**Figure 6b. Duplex Ampification Plot**
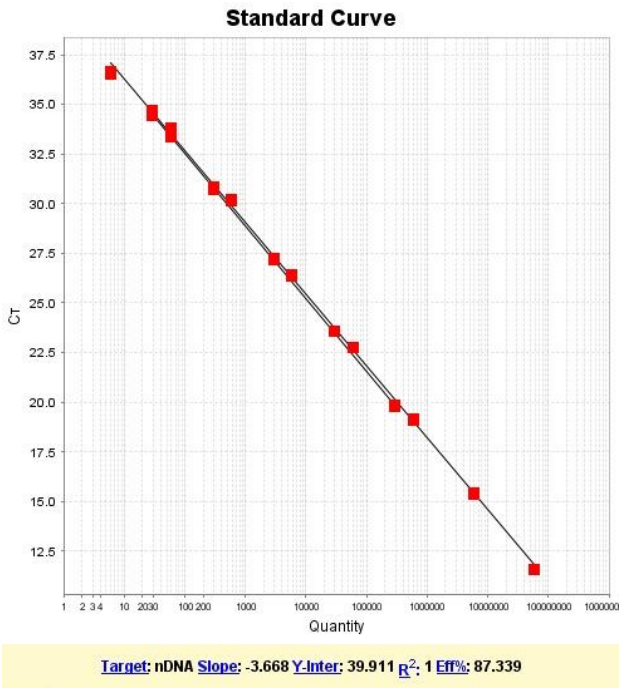	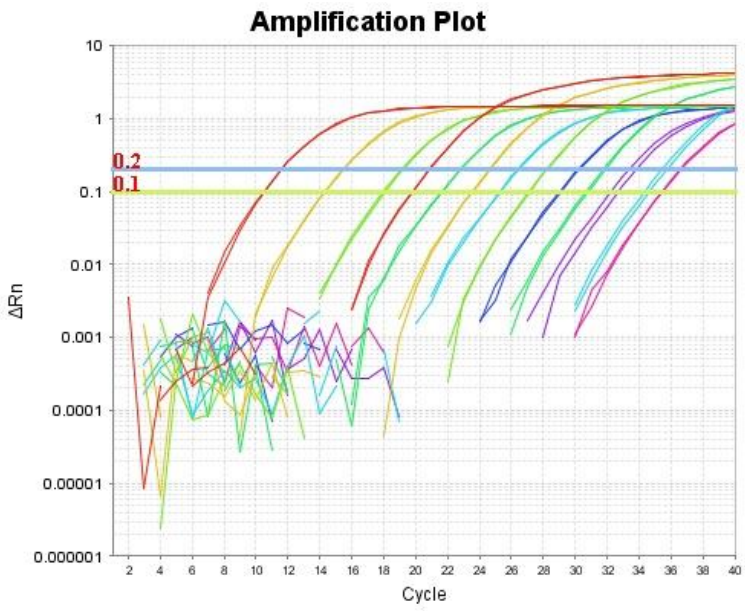
10X Dilution series of both targets (β2M and MinArc)	Per cycle amplification, the lower the cycle number for amplification the higher the quantity of sample or standard.

Analysis of accuracy is outlined in **Table 5a.** and **Table 5b.,** runs 7 through 9 used different concentrations than runs 10 through 12. The change in SRM concentration was due to the lower concentrations showing drastically different copy number ratios than expected.

Table 5a. Accuracy Analysis

SRM Component & Concentration (ng/μL)	Certified Ratios	Run 7	Run 8	Run 9
A 25	174 ± 4	113.5802418	130.0493338	120.0878293
A 2.5	174 ± 4	128.855986	131.704717	121.2069332
A 0.25	174 ± 4	306.1086491	116.9274614	133.3509707
A 0.025	174 ± 4	996.8109864	168.4748871	327.7959411
A 0.0025	174 ± 4	160.99049	76.73940567	165.2165168
B 25	206 ± 5	134.5071007	147.848997	141.8834021
B 2.5	206 ± 5	148.9777938	158.8154678	144.7757189
B 0.25	206 ± 5	765.178545	159.2176623	507.2598806
B 0.025	206 ± 5	236.9420359	282.421746	813.4436146
B 0.0025	206 ± 5	65.66244136	132.8281997	152.9014091
C 25	279 ± 7	194.3420971	211.278839	189.856953
C 2.5	279 ± 7	202.4277448	219.3111411	190.0289259
C 0.25	279 ± 7	229.2245257	242.4235162	198.6379543
C 0.025	279 ± 7	328.8259227	244.4748337	-
C 0.0025	279 ± 7	-	122.12136	106.1044879

mtDNA to nDNA ratios from copy number values. Boxes with no values recorded had nuclear drop out in both replicates. Rows highlighted red show inconsistent ratio estimates with the higher concentrations. Concentrations listed were used initially but changed for the last 3 runs because the accuracy drastically changed below 2.5ng/μL

Table 5b. Accuracy Analysis continued

SRM Component & Concentration (ng/μL)	Certified Ratios	Run 10	Run 11	Run 12
A 25	174 ± 4	112.34745	121.7673138	136.5325816
A 15	174 ± 4	108.5414445	119.1614617	131.6138633
A 10	174 ± 4	102.0655802	112.005922	127.4124709
A 5	174 ± 4	100.4146897	111.6267772	119.4168808
A 2.5	174 ± 4	96.88825516	110.1905039	122.8313093
B 25	206 ± 5	130.4134218	143.6046513	156.40518
B 15	206 ± 5	130.3816664	142.596688	161.486746
B 10	206 ± 5	129.6203734	141.5772067	153.7100602
B 5	206 ± 5	121.7041311	142.1269707	154.6348325
B 2.5	206 ± 5	116.0244636	135.481949	146.6942467
C 25	279 ± 7	186.4879029	199.2075623	218.6787045
C 15	279 ± 7	173.4265709	195.2643465	213.6112995
C 10	279 ± 7	179.7632435	199.7311034	216.5903871
C 5	279 ± 7	169.3410235	196.3075928	216.0888372
C 2.5	279 ± 7	171.0310509	203.2690888	212.585952

New SRM dilutions with concentrations ranging from 25ng/μL to 2.5ng/μL. mtDNA to nDNA ratios from copy number values.

Assay precision was assessed with Runs 7 through 12. The precision of the β2M standards was measured by cycle threshold values seen in **Table 6.** For each standard the average cycle threshold over the 6 runs was calculated in Excel along with the standard deviation, standard error, and confidence interval values for 90%, 95%, 99% and 99.9%. **Figure 7.** visualizes this data by showing the range, mean, and standard deviation in cycle threshold for each standard.

Table 6. β2M Only Standards Cycle Thresholds Precision Analysis

	STD1	STD2	STD3	STD4	STD5	STD6
Run 7	19.88507	23.79258	27.45842	31.17956	35.30622	36.36399
Run 7	19.86753	23.8416	27.63799	31.53831	34.90109	-
Run 8	19.73794	23.54636	26.95778	30.60759	33.66862	37.12268
Run 8	19.74820	23.4731	26.9444	30.59898	34.63679	36.80245
Run 9	19.81573	23.7085	27.61311	31.35147	35.7491	38.80727
Run 9	19.88432	23.75404	27.43204	31.37519	35.82389	-
Run 10	19.84462	23.58782	27.17645	30.87384	34.25219	38.60416
Run 10	19.93191	23.57252	27.18863	30.80154	-	38.89381
Run 11	19.82237	23.68102	27.28289	31.52488	35.07668	37.32308
Run 11	19.88699	23.77803	27.37752	30.88125	34.7769	37.89559
Run 12	19.81073	23.57682	27.16621	30.6918	34.43264	-
Run 12	19.83789	23.5991	27.21344	30.84124	34.71832	-
Avg	19.83944	23.65929	27.2874	31.02214	34.84931	37.72663
St Dev	0.057231	0.115779	0.224789	0.351662	0.633587	0.968593
St Error	0.016521	0.033423	0.064891	0.101516	0.191034	0.342449
CI 90	0.027177	0.05498	0.106746	0.166994	0.31425	0.563329
CI 95	0.032382	0.065508	0.127186	0.198971	0.374426	0.671201
CI 99	0.042559	0.086097	0.167159	0.261505	0.492103	0.88215
CI 99.9	0.054371	0.109994	0.213556	0.334089	0.628692	1.127001

CT values from each replicate of Standards 1-6 and the calculated Average (Avg), Standard Deviation (St Dev), Standard Error (St Error), and confidence intervals (CI). Boxes with no values recorded were due to drop out, which is expected at such low copy numbers.

Figure 7. Precision Analysis

Box and whisker plot of variation in cycle threshold for each standard, values from Table 6.

The precision of the MinArc standards was measured by cycle threshold values seen in **Table 7.** For each standard the average cycle threshold over the 6 runs was calculated in Excel along with the standard deviation, standard error, and confidence interval values for 90%, 95%, 99% and 99.9%. **Figure 8.** visualizes this data by showing the range, mean, and standard deviation in cycle threshold for each standard.

Table 7. MinArc Only Standards Cycle Threshold Precision Analysis

	STD1	STD2	STD3	STD4	STD5	STD6
Run 7	11.62071	15.52553	19.43729	23.17585	27.05026	30.80479
Run 7	11.18586	15.54454	19.47956	23.23606	27.02264	30.92162
Run 8	11.48819	15.37178	18.97353	22.65984	26.26009	29.96223
Run 8	11.5187	15.29103	18.97958	22.84978	26.24656	29.89326
Run 9	11.33207	15.29175	19.37042	23.31717	27.4852	31.834
Run 9	11.42917	15.34805	19.23915	23.33938	27.9814	32.21742
Run 10	11.05508	15.17536	18.90314	22.63054	26.22609	30.14195
Run 10	11.48397	15.17299	18.94325	22.6532	-	29.96569
Run 11	11.43822	15.36242	19.09939	23.17931	26.57614	30.4158
Run 11	11.5334	15.45569	19.15219	22.87335	26.59611	30.33593
Run 12	11.56946	15.38607	19.07212	22.74763	26.36772	30.12037
Run 12	11.57637	15.42345	19.14437	22.78352	26.43633	30.21884
Avg	11.43593	15.36239	19.1495	22.9538	26.74987	30.56933
St Dev	0.168282	0.118328	0.19545	0.274789	0.573386	0.754999
St Error	0.048579	0.034158	0.056422	0.079325	0.172882	0.217949
CI 90	0.079912	0.05619	0.092814	0.130489	0.284392	0.358527
CI 95	0.095214	0.06695	0.110586	0.155477	0.33885	0.427181
CI 99	0.125139	0.087992	0.145342	0.204341	0.445345	0.561437
CI 99.9	0.159873	0.112415	0.185684	0.261058	0.568956	0.717271

CT values from each replicate of Standards 1-6 and the calculated Average (Avg), Standard Deviation (St Dev), Standard Error (St Error), and confidence intervals (CI). Boxes with no values recorded were due to drop out.

Figure 8. Precision Analysis

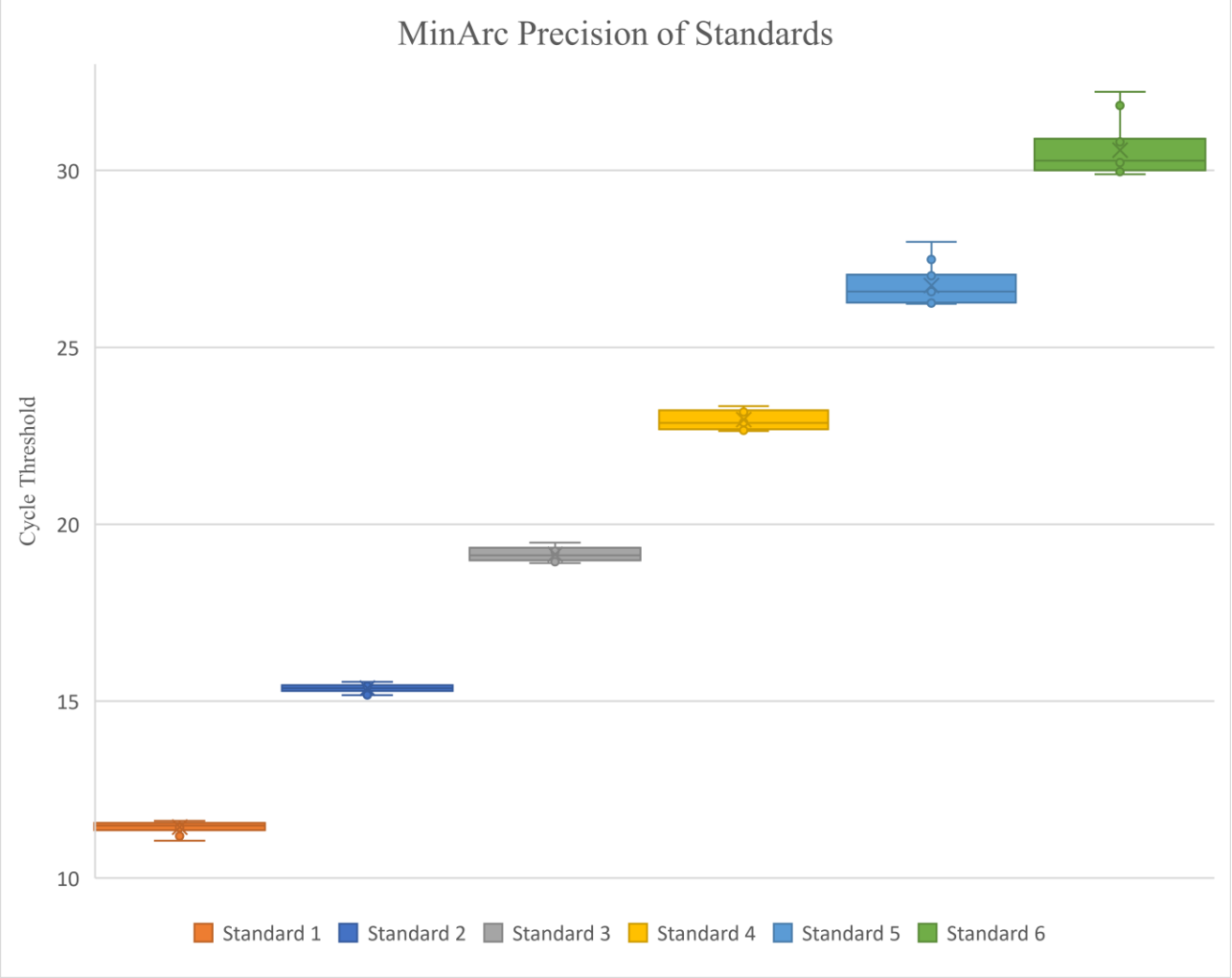

Box and whisker plot of variation in cycle threshold for each standard, values from Table 7.

V. Discussion:

There was little change in efficiency from singleplex to multiplex. It is generally regarded that an R^2 value above 0.98 is acceptable and efficiencies around 90-100% are considered high, especially for multiplex assays. The average efficiency of the duplex assay for both targets were in the mid 80%. There were 8 standards used but the last two often dropped out for nuclear quantification, as expected given the very limited copy number in these dilution series points and were deemed unnecessary henceforth.

The initial storage conditions for MinArc and β2M gBlock standards was at 1ng/μL and 0.1ng/μL, respectively, in a -20°C freezer. After several runs, the β2M copy number appeared to decrease while the MinArc remained consistent, shown in **Figure 5**. To test if the preparations of the standards caused this change, run 5 consisted of three sets: Set 1 repeated protocol from the previous run, set 2 standards were vortexed immediately before plating, and set 3 had the gBlocks heated to 95°C for 2 minutes before combining into the first standard as well as being vortexed before plating. There was not enough of a difference in cycle threshold to convince the need to adopt any of those changes in protocol. It was then found on the gBlock Gene Fragment's manufacturer "Frequently Ask Questions" page that storing

gBlocks at concentrations lower than 1ng/μL could result in a decrease in concentration due to the fragments irreversibly binding to the tube, even in low bind tubes. The β2M gBlock standards were remade from the primary stock and stored at 1ng/μL, then compared to gBlocks from the old method of storage. This brought the cycle threshold back to the expected value, and so all subsequent runs utilized the newly made gBlocks. The data in **Figure 5** is some of the first to show support of Integrated DNA Technologies claim of gBlocks irreversibly binding to the tube and decreasing in quantity when stored at too low of a concentration.

The accuracy of the assay did not perform as well as expected with respect to quantification results of known SRM materials. The observed ratios were lower than the expected ratios but did reproducibly follow the trend in that A had the lowest ratio, B in the middle, and C with the highest mtDNA to nDNA ratio (**Table 5a&b**). Due to the known shift in nuclear quantification from earlier runs, it was thought that the mtDNA copy number was closer to the actual values and the nDNA copy number was being over estimated. To attempt to mathematically correct for the apparent depletion in nDNA copy number, the copy number values were recalculated using the cycle threshold values and the standard curve equation from run 3, before the nDNA decreased in quantity (data not shown). The "corrected" values were still inaccurate and it was determined that the method should be re-evaluated. A more likely explanation is that it is a function of the differential nature of the standard DNA as compared to the SRM materials: the SRM components are made up of cellular DNA and are likely affected by dilution bias [**Malik et al. 2011**]. Dilution bias would also explain why the ratios varied much more drastically the more dilute the SRMs were. Further research into this observation is required.

The assessment of precision of the assay was separated into how consistently each standard quantified at certain cycle thresholds. The β2M component of the standards is displayed in **Table 6** and **Figure 7** and the MinArc component of the standards in **Table 7** and **Figure 8**. It appears that for both components the more dilute the standard the higher the standard deviation, more so in β2M. Overall the assay was deemed effectively reproducible due to the consistency over all 6 runs and the highest deviation being 0.969 cycle thresholds.. The data also indicates that more concentrated samples are more precisely quantified.

The optimization of this assay is ongoing due to the limited accuracy. The assay has proven to be precise and reproducible with sufficient efficiency. Possible future directions include sonication of samples and SRMs to examine if dilution bias could be the cause of inaccurate SRM quantification. Other methods of possibly reducing dilution bias mentioned in Malik *et al*. [**2011**] include manual shearing and the use of DNA carriers such as tRNA. Another avenue of future research could include a different method of mathematically correcting the data post run to improve accuracy.

There are a few limitations for consideration for use of the assay. Any deviations in protocol could potentially give misleading results due to the sensitive nature of the assay, specifically regarding mitochondrial DNA detection. Mitochondrial contamination of low TE is more easily detectable than nuclear contamination and both could negatively affect the standard curve, so it is recommended that before the creation of the standards that the low TE is UV crosslinked for at least 10 minutes. Proper storage of primers, probes, and gBlocks as well as limiting the number of freeze-thaws is also recommended for optimal assay use.

VI. Acknowledgements:

I thank Dr. Nicole Phillips for providing the equipment and materials used and for discussion. I also thank Dr. John V. Planz and Dr. Roxanne Zascavage for guidance and discussion. Thank you to Dr. Joseph Warren for the years of service to the Forensic Genetics Program at UNTHSC and for the mentorship he provided to his students throughout the program. I thank the NIH/NIMHD Administrative Supplement to U54 MD006882-08S2 for support of my time and effort on this project.

References

1. Alonso, A. (2004). Real-time PCR designs to estimate nuclear and mitochondrial DNA copy number in forensic and ancient DNA studies. *Forensic Science International*, *139*(2-3), 141–149. doi: 10.1016/j.forsciint.2003.10.008

2. Andréasson, H., Gyllensten, U., & Allen, M. (2002). Real-Time DNA Quantification of Nuclear and Mitochondrial DNA in Forensic Analysis. *BioTechniques*, *33*(2), 402–411. doi: 10.2144/02332rr07

3. Andréasson, H., Nilsson, M., Budowle, B., Lundberg, H., & Allen, M. (2006). Nuclear and mitochondrial DNA quantification of various forensic materials. *Forensic Science International*, *164*(1), 56–64. doi: 10.1016/j.forsciint.2005.11.024

4. Andreu, A. L., Martinez, R., Marti, R., & García-Arumí, E. (2009). Quantification of mitochondrial DNA copy number: Pre-analytical factors. *Mitochondrion*, *9*(4), 242–246. doi: 10.1016/j.mito.2009.02.006

5. Bai, R.-K., Perng, C.-L., Hsu, C.-H., & Wong, L.-J. C. (2004). Quantitative PCR Analysis of Mitochondrial DNA Content in Patients with Mitochondrial Disease. *Mitochondrial Pathogenesis*, 304–309. doi: 10.1007/978-3-662-41088-2_29

6. Bintz, B. J., Wilson, M. R. (n.d.) Development Of A Multiplex Quantitative PCR (qPCR) Assay For Simultaneous Quantification Of Human Nuclear And Mitochondrial DNA.

7. Bustin SA, Benes V, Garson JA, Hellemans J, Huggett J, Kubista M, Mueller R, Nolan T, Pfaffl MW, Shipley GL, Vandesompele J, Wittwer CT. The MIQE guidelines: minimum information for publication of quantitative real-time PCR experiments. Clin Chem. 2009;55:611–22.

8. Cavelier, L., Johannisson, A., & Gyllensten, U. (2000). Analysis of mtDNA Copy Number and Composition of Single Mitochondrial Particles Using Flow Cytometry and PCR. *Experimental Cell Research*, *259*(1), 79–85. doi: 10.1006/excr.2000.4949

9. Copy number calculator for realtime PCR. (n.d.). Retrieved from http://www.scienceprimer.com/copy-number-calculator-for-realtime-pcr

10. Dannenmann, B., Lehle, S., Lorscheid, S., Huber, S. M., Essmann, F., & Schulze-Osthoff, K. (2017). Simultaneous quantification of DNA damage and mitochondrial copy number by long-run DNA-damage quantification (LORD-Q). *Oncotarget*, *8*(68). doi: 10.18632/oncotarget.20112

11. Decker, A. E., Kline, M. C., Vallone, P. M., & Butler, J. M. (2005). Gaithersburg, MD.

12. Gonzalez-Hunt, C. P., Rooney, J. P., Ryde, I. T., Anbalagan, C., Joglekar, R., & Meyer, J. N. (2016). PCR-Based Analysis of Mitochondrial DNA Copy Number, Mitochondrial DNA Damage, and Nuclear DNA Damage. *Current Protocols in Toxicology*. doi: 10.1002/0471140856.tx2011s67

13. Jayaprakash, A. D., Benson, E. K., Gone, S., Liang, R., Shim, J., Lambertini, L., … Sachidanandam, R. (2015). Stable heteroplasmy at the single-cell level is facilitated by intercellular exchange of mtDNA. *Nucleic Acids Research*, *43*(4), 2177–2187. doi: 10.1093/nar/gkv052

14. Kanagawa, T. (2003). Bias and artifacts in multitemplate polymerase chain reactions (PCR). *Journal of Bioscience and Bioengineering*, *96*(4), 317–323. doi: 10.1016/s1389-1723(03)90130-7

15. Kavlick, M. F. (2019). Development of a triplex mtDNA qPCR assay to assess quantification, degradation, inhibition, and amplification target copy numbers. *Mitochondrion*, *46*, 41–50. doi: 10.1016/j.mito.2018.09.007

16. Kavlick, M. F., Lawrence, H. S., Merritt, R. T., Fisher, C., Isenberg, A., Robertson, J. M., & Budowle, B. (2011). Quantification of Human Mitochondrial DNA Using Synthesized DNA Standards*. *Journal of Forensic Sciences*, *56*(6), 1457–1463. doi: 10.1111/j.1556-4029.2011.01871.x

17. Livak, K. J., & Schmittgen, T. D. (2001). Analysis of Relative Gene Expression Data Using Real-Time Quantitative PCR and the 2−ΔΔCT Method. *Methods*, *25*(4), 402–408. doi: 10.1006/meth.2001.1262

18. Malik, A. N., & Czajka, A. (2013). Is mitochondrial DNA content a potential biomarker of mitochondrial dysfunction? *Mitochondrion*, *13*(5), 481–492. doi: 10.1016/j.mito.2012.10.011

19. Malik, A. N., Shahni, R., Rodriguez-De-Ledesma, A., Laftah, A., & Cunningham, P. (2011). Mitochondrial DNA as a non-invasive biomarker: Accurate quantification using real time quantitative PCR without co-amplification of pseudogenes and dilution bias. *Biochemical and Biophysical Research Communications*, *412*(1), 1–7. doi: 10.1016/j.bbrc.2011.06.067

20. Meissner, C., Mohamed, S., Klueter, H., Hamann, K., Wurmb, N. V., & Oehmichen, M. (2000). Quantification of mitochondrial DNA in human blood cells using an automated detection system. *Forensic Science International*, *113*(1-3), 109–112. doi: 10.1016/s0379-0738(00)00249-8

21. Phillips, N. R., Sprouse, M. L., & Roby, R. K. (2014). Simultaneous quantification of mitochondrial DNA copy number and deletion ratio: A multiplex real-time PCR assay. *Scientific Reports*, *4*(1). doi: 10.1038/srep03887

22. Romsos, E. L., Kline, M. C., Duewer, D. L., Toman, B., & Farkas, N. (2018). Certification of standard reference material 2372a human DNA quantitation standard. doi: 10.6028/nist.sp.260-189

23. Rooney, J. P., Ryde, I. T., Sanders, L. H., Howlett, E. H., Colton, M. D., Germ, K. E., … Meyer, J. N. (2014). PCR Based Determination of Mitochondrial DNA Copy Number in Multiple Species. *Methods in Molecular Biology Mitochondrial Regulation*, 23–38. doi: 10.1007/978-1-4939-1875-1_3

24. Shmookler Reis, R. J., & Goldstein, S. J. (1983). Mitochondrial DNA in Mortal and Immortal Human Cell. *The Journal of Biological Chemistry*, *258*(15). doi: http://www.jbc.org/

25. Spelbrink, J. N. (2009). Functional organization of mammalian mitochondrial DNA in nucleoids: History, recent developments, and future challenges. *IUBMB Life*. doi: 10.1002/iub.282

26. Timken, M. D., Swango, K. L., Orrego, C., & Buoncristiani, M. R. (2005). A Duplex Real-Time qPCR Assay for the Quantification of Human Nuclear and Mitochondrial DNA in Forensic Samples: Implications for Quantifying DNA in Degraded Samples. *Journal of Forensic Sciences*, *50*(5), 1–17. doi: 10.1520/jfs2004423

27. Wallace, D. C. (2010). Mitochondrial DNA Mutations in Disease and Aging. *Environmental and Molecular Mutagenesis*, 51:440-450. Doi: 10.1002/em

28. Wurmb-Schwark, N. V., Higuchi, R., Fenech, A., Elfstroem, C., Meissner, C., Oehmichen, M., & Cortopassi, G. (2002). Quantification of human mitochondrial DNA in a real time PCR. *Forensic Science International*, *126*(1), 34–39. doi: 10.1016/s0379-0738(02)00026-9

29. Wurmb-Schwark, N. V., Schwark, T., Harbeck, M., & Oehmichen, M. (2004). A simple Duplex-PCR to evaluate the DNA quality of anthropological and forensic samples prior short tandem repeat typing. *Legal Medicine*, *6*(2), 80–88. doi: 10.1016/j.legalmed.2003.10.002

30. Zhang, H., Cooney, D. A., Sreenath, A., Zhan, Q., Agbaria, R., Stowe, E. E., … Johns, D. G. (1994). Quantitation of Mitochondrial DNA in Human Lymphoblasts by a Competitive Polymerase Chain Reaction Method: Application to the Study of Inhibitors of Mitochondrial DNA Content. *The American Society for Pharmacology and Experimental Therapeutics*. doi: 0026-895X/94/061063-07

VII. Summary

The goal of this internship project was to optimize and evaluate an absolute real-time quantitative PCR (qPCR) Duplex Assay for the precise and accurate quantification of mitochondrial DNA (mtDNA) and nuclear DNA (nDNA). The optimization of this qPCR Duplex Assay allows for the simultaneous quantification of mtDNA and nDNA in a sample; the ratio of the two components can be used to estimate mitochondrial DNA copy number, also referred to as "mtDNA content" [**Bai et al., 2004]**. In forensics, copy number data can be used for determining the type of analysis to perform based on the state of degradation and if, mtDNA should be tested in place of nDNA in order to conserve resources and limited samples [**Alonso et al., 2004; Andréasson et al., 2002 & 2006, Bintz & Wilson, n.d.; Meissner et al., 2000; Timken et al, 2005; Wurmb-Schwark et al., 2002 & 2004**]. In biomedical research, mtDNA content can be used to indicate overall mitochondrial health, observe ratio changes in various tissue types following treatment, and to examine metabolic mechanisms [**Bai et al., 2004; Dennenmann et al., 2017; Gonzalez-Hunt et al., 2016; Wallace, 2010; Rooney et al., 2014**]. The protocol developed from this project has applications in a wide variety of research projects.

To carry out optimization, the use of synthetic oligomer standards "gBlocks Gene Fragments" from Integrated DNA Technologies was applied. Using a gBlock standard was advantageous because the sequences were synthesized double stranded and thus limited the chance of any self-interaction and more closely mimicked DNA *in vivo*. The nuclear target and the mitochondrial target did not interfere with one another and amplified under similar conditions. Absolute qPCR was used because it utilizes a standard curve which allows for the direct comparison of unknowns to obtain a copy number rather than relying on a reference gene or sample as is used in relative qPCR [**Rooney et al., 2014; Andreu et al., 2009; Bai et al., 2004**]. Modeling after the Phillips *et al*. assay, the mitochondrial target was a site in the minor arc (MinArc) from nucleotide position 16,528 to 43, and the nuclear target was a single copy locus on Chromosome 15 (β2M) from nucleotide position 15,798,932 to 15,799,026. The same primer and probe designs were utilized. A singleplex preliminary assay for each target was run to ensure the amplification of each gBlock, to establish individual accuracy and efficiency, and to observe if either change when multiplexed. It was demonstrated that the standards work with the primers and probes for both mtDNA and nDNA separately and were subsequently duplexed. The duplex master mix design that was optimal included a per reaction composition of 12.5μL of *Taq* Universal Master Mix (ThermoFisher Scientific), 2μL of each β2M primer at 7.5μM, 1.25μL of β2M probe at 4μM, 2μL of each MinArc primer at 625nM, and 1.25μL of MinArc probe at 2μM. This design resulted in high R^2 values for the standards as well as sufficiently high efficiencies. The precision of the assay was analyzed over 6 replicated runs and was deemed effectively reproducible. The accuracy was assessed with the use of a standard reference material (SRM 2372a) and was found to be problematic [**Romsos et al., 2018**]. This could be from a possible dilution bias of the SRM, effectively changing the copy number ratios in a difficult to predict way. An attempt to mathematically correct the data was made but did not provide any solution. Future directions include sonication of the SRM to examine if dilution bias could be the cause of the inaccuracy observed as well as continuing research into other methods of mathematically correcting the data for improved accuracy.